doi.org/10.1002/cbdv.202200695

RESEARCH ARTICLE

CHEMISTRY & BIODIVERSITY

Oxoplatin-Based Pt(IV) Lipoate Complexes and Their Biological Activity

Xiao Liu[+,a] Marie-Christin Barth[+,a] Klaudia Cseh,[b] Christian R. Kowol,[b] Michael A. Jakupec,[b, c] Bernhard K. Keppler,*[b, c] Dan Gibson,*[d] and Wolfgang Weigand*[a]

[a] Institute of Inorganic and Analytical, Friedrich Schiller University Jena, Humboldtstrasse 8, 07743 Jena, Germany, e-mail: wolfgang.weigand@uni-jena.de
[b] Institute of Inorganic Chemistry, Faculty of Chemistry, University of Vienna, Währinger Strasse 42, A-1090 Vienna, Austria, e-mail: bernhard.keppler@univie.ac.at
[c] Research Cluster 'Translational Cancer Therapy Research', University of Vienna, Währinger Strasse 42, A-1090 Vienna, Austria
[d] Institute for Drug Research, School of Pharmacy, The Hebrew University of Jerusalem, Jerusalem, 9112102, Israel, e-mail: dang@ekmd.huji.ac.il

α-Lipoic acid, known for its anti-inflammatory and antioxidant activity, represents a promising ligand for Pt(IV) prodrugs. Three new Pt(IV) lipoate complexes were synthesized and characterized by NMR spectroscopy (^{1}H, ^{13}C, ^{195}Pt), mass spectrometry and elemental analysis. Due to the low solubility of the complex containing two axial lipoate ligands, further experiments to examine the biological activity were performed with two Pt(IV) complexes containing just one axial lipoate ligand. Both complexes exhibit anticancer activity and produce reactive oxygen species (ROS) in the cell lines tested. Especially, the monosubstituted complex can be reduced by ascorbic acid and forms adducts with 9-methylguanine (9MeG), which is favorable for the formation of DNA-crosslinks in the cells.

Keywords: lipoic acid, Pt(IV) prodrugs, multi-action, cyclovoltammetry, ROS.

Introduction

α-Lipoic acid (ALA), first isolated and characterized by Lester Reed and coworkers in 1951,[1] has been extensively studied for pharmaceutical and nutraceutical potentials regarding its antioxidant and anti-inflammatory properties.[2–5] Besides the regulation of the redox status in cells through thiol/disulfide exchange reactions,[3,6,7] ALA acts as an essential cofactor for α-ketoacid dehydrogenase complexes (e.g., pyruvate dehydrogenase, PDH) in the cellular energy metabolism.[8,9] The activity of PDH, which catalyzes the oxidative carboxylation of pyruvate in the mitochondria and thereby bridges the anaerobic and aerobic metabolism,[9,10] can be enhanced by ALA supplementation.[11] The previous mentioned characteristics of ALA contribute to the reported inhibition of proliferation in various cancer cell lines, which feature inefficient aerobic glycolysis ('Warburg effect') and oxidative stress.[4,6,10,12] Apart from that, ALA was referred to have beneficial protective effects on chemotherapy-induced side-effects,[13–15] nevertheless additional clinical trials need to be conducted.

Metal-based anticancer agents, especially Pt(II) complexes approved by the Food and Drug Administration (cisplatin, carboplatin, oxaliplatin) have shown excellent efficacy in the treatment of numerous types of carcinomas all over the world.[16–18] Despite Pt-based drugs' documented medical success, adverse effects such as nephro-, cardio- or neurotoxicity as well as intrinsic and acquired resistance mechanisms

[+] These authors contributed equally to this work.

Supporting information for this article is available on the WWW under https://doi.org/10.1002/cbdv.202200695

still restrain their application.[19–21] To overcome the frontiers of Pt(II) anticancer agents, octahedral Pt(IV) complexes with two additional axial ligands, synthesized by additive oxidation to cisplatin and its analogs, might enhance drug efficiency and decrease severe side-effects during therapy. Due to their higher kinetic stability compared to that of Pt(II), Pt(IV) prodrugs are believed to remain intact before entering the cells and are activated by intracellular reduction releasing the cytotoxic Pt(II) species and the free axial ligands.[22–25] Following the aquation of the released Pt(II) species, reactive Pt(II) metabolites attack and distort the cancer cell DNA, initiating cell death if the DNA damages cannot be repaired.[19,20,26] Bioactive axial ligands can influence the pharmacological characteristics of the drug as well as circumvent cisplatin resistance.[24,26,27] One example of bioactive ligands displays phenylbutyric acid (PhB), an inhibitor auf histone deacetylases, which affect epigenetic mechanisms and are known to have anticancer activity.[28–30] The introduction of phenyl butyrate ligands as inhibitor of histone deacetylases was already shown to enhance the cytotoxicity of Pt(IV) complexes compared to cisplatin.[28] In the literature, Pt(IV) lipoate complexes based on kiteplatin have already shown promising anticancer activity *in vitro*.[31]

Herein, we describe the synthesis and characterization of three Pt(IV) lipoate complexes based on cisplatin (*Scheme 1*). Two of them were further analyzed for their stability, reduction behavior in presence of ascorbic acid and electrochemical properties. Their interaction with a DNA model, the cytotoxicity against different cancer cell lines as well as their ability to produce reactive oxygen species were examined.

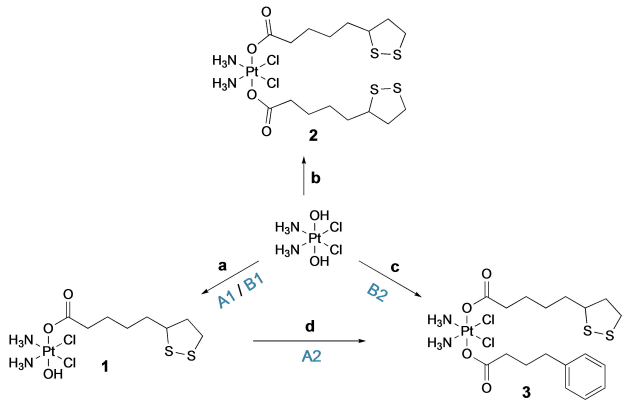

Scheme 1. Synthetic routes of Pt(IV) lipoate complexes **1**–**3**. Reactants and conditions: a) Method A1: ALA-NHS (1.05 equiv.), DMSO, 50 °C, overnight; method B1: ALA anhydride (0.91 equiv.), DMF, r.t., overnight; b) ALA anhydride (4 equiv.), DMF, r.t., 2 d; c) Method B2: i) PhB anhydride (0.95 equiv.), DMSO, r.t., overnight; ii) ALA anhydride (4 equiv.), DMF, r.t., 3 d; d) method A2: PhB anhydride (4 equiv.), DMF, r.t., overnight.

Results and Discussion

Synthesis and Characterization

Cisplatin was prepared according to previously published procedures with slight modifications.[32] The corresponding Pt(IV) precursor, oxoplatin, was obtained by oxidation with hydrogen peroxide solution (w/w, 30 %).[33] Two different synthesis strategies were used to prepare monofunctional lipoate complex **1**. On the one hand, commercially available ALA was activated into its succinimide ester (ALA-NHS),[34] on the other hand, ALA anhydride was formed using *N*,*N*′-dicyclohexylcarbodiimide (DCC) as coupling agent.[35] Subsequently, oxoplatin was reacted with ALA-NHS (method A1) in DMSO or ALA anhydride (method B1) in DMF to yield complex **1**, respectively (*Scheme 1*). Here, complex **1** was mainly synthesized using method B1, since the reaction could be performed at room temperature and DMF can be removed by rotary evaporation. The reaction of oxoplatin with an excess of ALA anhydride yielded the disubstituted Pt(IV) complex **2** (*Scheme 1*). The 'triple-action' Pt(IV) complex **3** is synthesized by a reaction of complex **1** with PhB anhydride in DMF (method A2).

In an alternative route, **3** can be prepared by the synthesis of the monofunctional Pt(IV) phenylbutyrate complex and the following reaction with ALA anhydride (method B2). However, due to longer reaction times and lower yield of method B2 compared to method A2, we usually applied method A2 for the synthesis of complex **3**.

All complexes were characterized by nuclear magnetic resonance (NMR) spectroscopy, electrospray ionization mass spectrometry (ESI-MS) and elemental analysis. The ESI mass spectra show the deprotonated molecular ions of all complexes (*Figures S1*, *S4*, *S8*), the found isotopic patterns accord with the theoretical ones.

The proton resonances of the ammine coordinated to the Pt(IV) center of **1** appeared over a wide range from 5.83 to 6.09 ppm, which is in good agreement with literature reports.[36] A full assignment of ^{1}H shifts to the lipoate moiety was accomplished by using ^{1}H-^{1}H correlation spectroscopy (COSY) NMR measurements (*Figure S2*). The methylene protons (H1, see numbering of protons in *Figure S2*) of coordinated ALA

showed a triplet at 2.16 ppm. Two multiplets at 1.48 and 1.38 ppm were assigned to the methylene protons H2 und H3. The multiplets located at 1.65 and 1.53 ppm were attributed to two protons (H4). The proton signal resonating at 3.60 ppm was assigned to the CH of H5 based on a COSY cross peak with the protons of H4 and two additional cross peaks with the multiplets resonating at 2.42 and 1.88 ppm, which were dedicated to the methylene protons H6, respectively. The last multiplet with an integration of two protons at 3.16 ppm belongs to the methylene protons of the 1,2-dithiolane ring at H7.

The proton resonance signals of the symmetrical disubstituted complex **2** differ slightly from the signals of the monosubstituted complex **1**, because the axial hydroxido ligand of **1** causes a different chemical environment than the axial lipoate ligand. Due to the low solubility of complex **2**, it was excluded from further studies.

The proton resonances of the ammine coordinated to the Pt(IV) center of complex **3** appeared downshifted to 6.5 ppm, compared to those of complex **1**.[36] As the proton resonances of the lipoate moiety in complex **3** are basically coincident with those of complex **1**, thus only proton assignments of PhB were described here. Signals in the aromatic region of the NMR spectrum of **3** with a range of 7.29–7.15 ppm were assigned to five protons of the phenyl group (H11), while the triplet at 2.59 ppm was assigned to the methylene group (H10) attached to the phenyl group (*Figure S5*). Multiplets from 2.25 to 2.20 ppm were assigned to the methylene groups next to the carboxylic groups of lipoate (H1) and phenylbutyrate (H8), respectively. The methylene protons H9 of phenylbutyrate are shown at 1.75 ppm, overlapping with the protons from lipoate (H4).

Stability Study

The stabilities of complexes **1** and **3** were evaluated using $^{195}Pt\{^{1}H\}$ NMR spectrometry in a solution of mixed DMSO-phosphate-saline buffer (PBS, pH 7.4; 4:1) at 37 °C. After 96 h, signals of 1026 ppm for **1** and 1205 ppm for **3** were found and no signals were observed in the range of −1000 to −4000 ppm typically for Pt(II) species, which suggested that complexes **1** and **3** are stable under these conditions over 96 h (*Figure S9*).

Electrochemistry

Acting as prodrugs, biologically active Pt(II) species need to be released after intracellular reduction of Pt(IV) complexes, rendering the reduction potential of Pt(IV) prodrugs a crucial pharmacological parameter. Thus, complexes **1** and **3** were investigated by cyclic voltammetry in DMF solution at a scan rate of 200 mV s^{-1} using 0.10 M [n-Bu$_4$N][PF$_6$] as supporting electrolyte. [Fe(η^5-C$_5$H$_5$)$_2$] (Fc/Fc$^+$) was used as the internal standard. The cyclic voltammograms of those two compounds are displayed in *Figure 1*. Both complexes **1** and **3** showed a reduction peak (−2.50 V) relating to the reduction of S–S bond, which was in accordance with that of the free ligand ALA (*Figure S10*). Complexes **1** and **3** displayed one irreversible reduction peak corresponding to Pt(II/IV) reduction at −1.43 V and −1.28 V, respectively. The monofunctional complex **1** showed a more negative reduction potential of Pt(II/IV) than that of complex **3**, which is consistent with reported literatures.[37,38]

Reduction Rate in the Presence of Ascorbic Acid

Unfortunately, there is no direct correlation between the reduction potentials and reduction rates of Pt(IV) complexes.[37,39] Therefore, the reduction rate in the presence of ascorbic acid (AsA; 5 equiv.) was investigated for complexes **1** and **3**. Due to the limited water solubilities of both complexes, the reduction study was investigated in a mixture of DMF and PBS (pH 7.4; 4:1) at 37 °C over 24 h. The reaction progress was monitored by $^{195}Pt\{^{1}H\}$ NMR spectroscopy.

As shown in *Figure 2*, the ^{195}Pt signal of complex **1** disappeared after incubation for 24 h, while a peak at −2096 ppm was detected and assigned to cisplatin. The reduction rate of complex **3** is significantly slower than that of **1**, as the signal at 1229 ppm was still

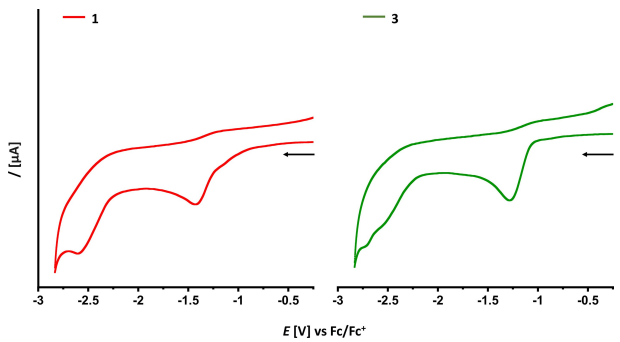

Figure 1. The cyclic voltammograms of **1** and **3** (1 mM) in 0.1 M DMF-[n-Bu$_4$N][PF$_6$] at a scan rate of 0.2 V s^{-1}.

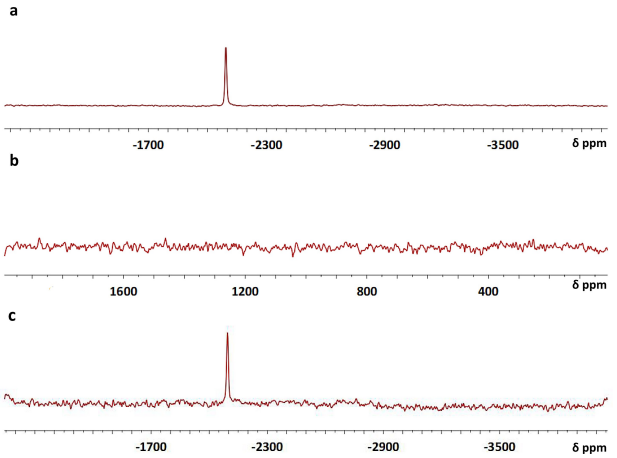

Figure 2. $^{195}Pt\{^{1}H\}$ NMR spectra of a) cisplatin in DMF-PBS (pH 7.4; 4:1); b) and c) complex **1** (16 mM) and AsA (5 equiv.) in DMF-PBS (pH 7.4; 4:1) with an incubation period of 24 h at 37 °C.

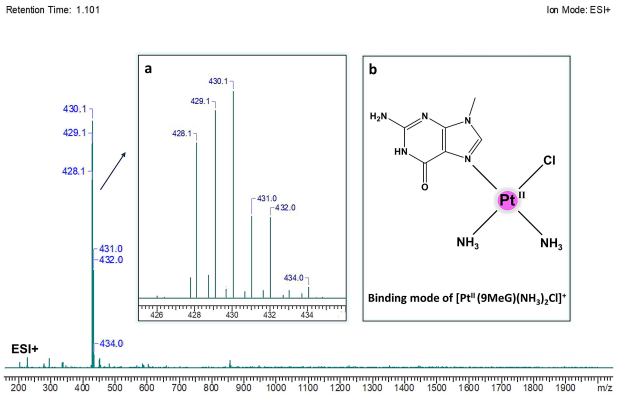

Figure 3. LC-ESI-MS of the reaction of complex **1** with 9MeG in the presence of AsA in DMF-PBS (pH 7.4; 4:1) after 20 h. The insets show: a) The isotope pattern of *m/z* 430.1, assigned to $[C_6H_{13}N_7OClPt]^+$; b) The binding mode of $[Pt^{II}(9MeG)(NH_3)_2Cl]^+$.

observed after an incubation time of 24 h. Also, no peak around −2000 ppm was detected, demonstrating no or marginal reduction happened (*Figure S11a*). Even the addition of further 10 equiv. AsA and extension of the incubation time to 48 h, the reduction was not complete (*Figure S11b*). In general, the coordination sphere of the Pt(IV) ion influences the reduction rate of the complexes. In contrast to disubstituted Pt(IV) complexes, monosubstituted Pt(IV) complexes are easier reduced by ascorbic acid, since the hydroxido ligand facilitates the electron transfer from the reducing agent to the Pt(IV) center.[36,37,40]

DNA Interaction

The generally accepted mechanism of action of cisplatin involves the formation of Pt-DNA adducts via covalent binding of a Pt(II) species with purine bases, particularly the N7 position of guanine.[19,26] Complex **1** can be reduced and thereby activated by AsA, since the signal for Pt(IV) disappeared in the $^{195}Pt\{^{1}H\}$ NMR spectrum (*Figure 2b*). To check its redox stability and DNA interaction, we investigated the reaction of complex **1** and 9MeG as DNA model with prior reduction by excess of AsA in DMF-PBS (pH 7.4; 4:1) at 37 °C. The reaction was analyzed by LC-ESI-MS for postulation of the species formed. The ESI-spectrum shows species with *m/z* 430.1 (t_R = 1.10 min, *Figure 3*) and *m/z* 578.0 (t_R = 1.80 min, *Figure S12*), that can be assigned to the complexes $[Pt^{II}(9MeG)(NH_3)_2Cl]^+$ and $[Pt^{II}(9MeG)_2(NH_3)Cl]^+$, respectively.

Moreover, the two Pt(II) species can be found coordinated with acetonitrile (*m/z* 470.8 and *m/z* 618.8, *Figures S13*, *S14*), which is used as eluent in the LC-ESI-MS. To confirm the general formation of Pt^{II}-9MeG adducts, the reaction was repeated with cisplatin and 3 equiv. 9MeG. The retention times and the species formed correspond to the previous experiment (*Figures S15*, *S16*).

Biological Activity

The complexes **1** and **3**, lipoic acid and a referential mixture of cisplatin and lipoic acid (1:1) were tested on their cytotoxicity in SW480 (colon carcinoma), A549 (non-small-cell lung carcinoma) and CH1/PA-1 (ovarian teratocarcinoma) cells. Complexes **1** and **3** were dissolved in DMSO, cisplatin and lipoic acid in supplemented MEM, and all were serially diluted in MEM. Due to the low activity of ALA, its examined concentration range was extended to 800 µM. After an incubation time of 96 h at 37 °C, concentration-effect curves were obtained by the MTT assay from at least three independent experiments (*Figure 4*). The assay measures the metabolic activity of cells by reduction of the MTT dye to formazan crystals, which usually correlates directly with the number of viable cells.[41,42] ALA, which is known for its antiproliferative effects in cancer cells[43–45] has shown the highest IC_{50} and thereby the lowest potency (*Table 1*). Both Pt(IV) complexes show (at least slightly) lower IC_{50} values than cisplatin. Furthermore, **3** with the axial bioactive phenyl butyrate ligand (histone deacetylase inhibitor) seems to be slightly though not significantly more cytotoxic than **1** in CH1/PA-1 cells. Taking into

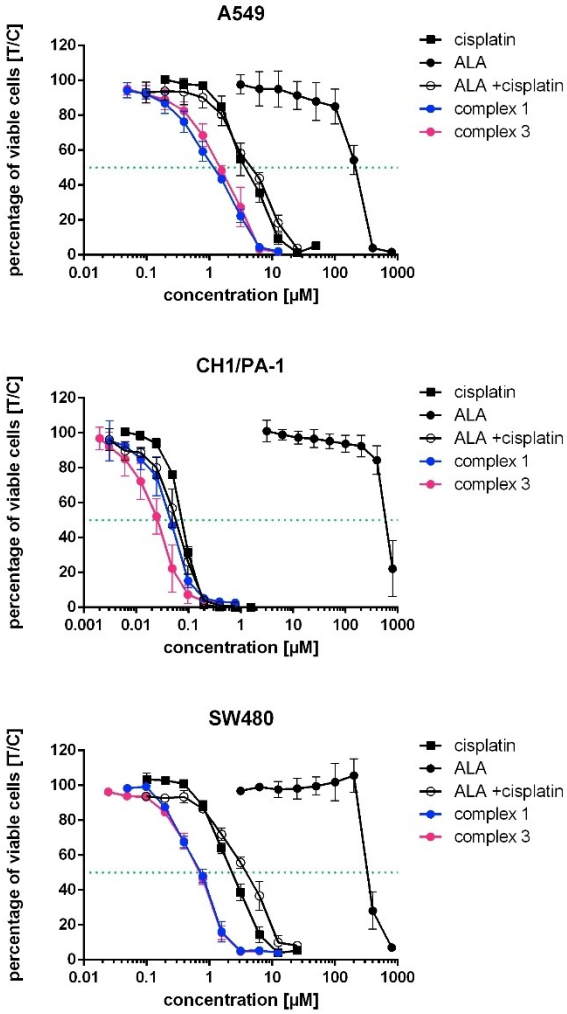

Figure 4. Concentration-effect curves of complexes **1** and **3**, ALA and ALA + cisplatin compared to cisplatin in the MTT assay (96 h exposure) in three human cancer cell lines A549, CH1/PA-1 and SW480.

consideration the high cytotoxicity of the Pt(IV) complexes compared to the referential Pt(II) complex cisplatin, the question arose if the coordination bond of the Pt(IV) center and ALA has an influence on the activity of the prodrugs. That is why a 1:1 mixture of ALA and cisplatin was also tested by means of the MTT assay (*Table 1*). The combination of cisplatin and ALA turned out to have similar cytotoxicity to cisplatin in SW480 and A549 cells with IC_{50} values of 4.0 μM and 4.7 μM, respectively. This is not surprising considering the low cytotoxicity of ALA which is probably due to its inability to penetrate cancer cells efficiently due to its polarity. Remarkably, the IC_{50} values of ALA + cisplatin and **1** are similar in CH1/PA-1 cells.

Since ALA is known as a biological antioxidant in cells,[46,47] but also for its prooxidative properties,[48,49] the generation of reactive oxygen species (ROS) by Pt(IV) lipoate complexes was of special interest. The excessive occurrence of ROS, e.g., H_2O_2, HO· or O_2^-, causes oxidative stress in cells, leading to damage of lipids, proteins and nucleic acids as well as cell death.[50,51] Pt drugs are known to induce ROS triggering apoptosis,[52–54] while ROS can also be associated with resistance mechanisms hampering the antitumor activity of the drugs.[55,56] The ROS assay uses non-fluorescent 2′,7′-dichloro-dihydrofluorescein diacetate (DCFH-DA), which enters the cells, is hydrolyzed by cellular esterases and reacts with ROS under conversion to fluorescent 2′,7′-dichloro-fluorescein (DCF) that can be detected.[57] Complexes **1** and **3** were tested in four different concentrations from 3.125 to 200 μM in equal steps. The relative fluorescence intensity measured over time for the complexes is summarized in *Figure 5*.

Complexes **1** and **3** can both induce ROS generation up to 4- and 3.5-fold, respectively, but only when concentrations manifold higher than the long-term IC_{50} values (according to the 96 h MTT assay reported above) are applied. The axial hydroxido ligand of the mono-substituted complex facilitate the induction of ROS.[39]

Conclusions

Three Pt(IV) lipoate complexes **1**–**3** were prepared and thoroughly characterized by means of spectroscopic

Table 1. Cytotoxicity values of complexes **1** and **3**, ALA and ALA + cisplatin (1:1) compared to cisplatin (mean IC_{50} values ± standard deviations in μM in the MTT assay, 96 h exposure).

Compound	CH1/PA-1	SW480	A549
Complex **1**	0.045 ± 0.002	0.74 ± 0.08	1.1 ± 0.1
Complex **3**	0.027 ± 0.009	0.70 ± 0.08	1.5 ± 0.2
ALA	597 ± 79	331 ± 24	212 ± 22
ALA + cisplatin	0.057 ± 0.012	4.0 ± 0.8	4.7 ± 0.4
cisplatin	0.073 ± 0.001	2.3 ± 0.2	3.8 ± 1.0

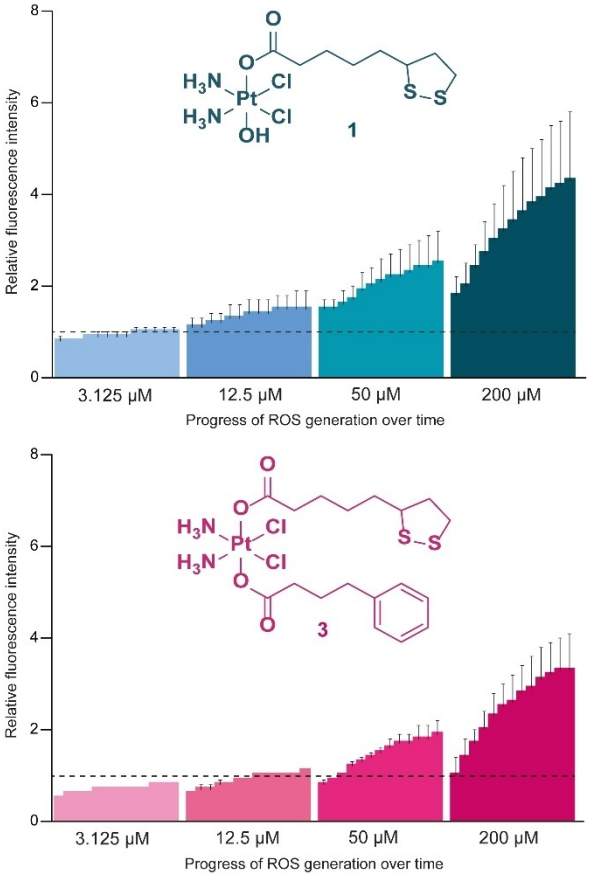

Figure 5. ROS induction in SW480 cells by complexes **1** (top) and **3** (bottom) in different concentrations over time for up to 2 h. Values are normalized to the untreated, negative control. The negative control level is indicated with the dashed line.

and spectrometric techniques. The *in vitro* cytotoxicity of **1** and **3** was tested on a panel of three human cancer cell lines. Complex **1** exhibits a more negative reduction potential than that of **3**, however, complex **1** can be reduced by AsA faster than **3**, thus, no correlation between reduction potentials and the ease of reduction with AsA was observed. Through the reaction of 9MeG and complex **1**, Pt^{II}-9MeG adducts were observed by use of mass spectrometry. Hence, after intracellular reduction, the activated Pt(II) species can attack the DNA strands, resulting in the formation of Pt^{II}-DNA crosslinks. Treatment of SW480 cells with **1** and **3** showed an increase in cellular ROS production applying fourfold concentrations with respect to the observed IC_{50} values.

Experimental Section

Materials and Methods

All reagents and solvents were of analytical grade and were used as received without further purification. K_2PtCl_4 was donated from Umicore AG & Co. KG Hanau-Wolfgang. α-Lipoic acid was obtained from abcr GmbH. DCC was purchased from Carl Roth GmbH. NHS was purchased from TCI Deutschland GmbH. 4-Phenylbutyrate acid, anhydrous DMSO and anhydrous DMF were obtained from Sigma–Aldrich and Alfa Aesar Thermo Fisher Scientific, respectively. The $^{1}H,^{13}C\{^{1}H\}$ and $^{195}Pt\{^{1}H\}$ NMR spectra were recorded with a Bruker Avance 400 MHz spectrometer. Chemical shifts are given in parts per million with references to internal $SiMe_4$ (^{1}H, ^{13}C) or to external K_2PtCl_4 (^{195}Pt). The mass spectra were recorded with Bruker (Bremen, Germany) MAXIS mass spectrometer. Elemental analysis was performed with a Leco CHNS-932 apparatus. TLC was performed by using Merck TLC aluminum sheets (silica gel 60 F254). Geduran Si 60 (0.063–0.200 mm) was used as the stationary phase for column chromatography.

Synthesis of Compounds

ALA-NHS

To a solution of lipoic acid (100 mg, 0.48 mmol) in 7 ml of acetonitrile, *N*-hydroxysuccinimide (NHS, 78 mg, 0.68 mmol) and 1-Ethyl-3-(3-dimethylamino-propyl) carbodiimide hydrochloride (EDC·HCl, 122 mg, 0.63 mmol) were added. The mixture was kept stirring overnight at room temperature. After reaction, the solvent was removed by reduced pressure and the residue was dissolved in dichloromethane (15 ml). The resulted solution was washed with a saturated solution of $NaHCO_3$, dried over anhydrous Na_2SO_4 and evaporated in vacuum to obtain a yellow solid (140 mg, 95%). ^{1}H-NMR (400 MHz, $CDCl_3$): δ 3.62–3.55 (m, 1H, -CH-), 3.18–3.12 (m, 2H), 2.84 (br. s, 4H, CO-CH_2CH_2-CO), 2.63 (t, $J=7.3$, 2H, -CH_2-CO), 2.48–2.45 (m, 1H), 1.95–1.88 (m, 1H), 1.83–1.50 (m, 6H) ppm. $^{13}C\{^{1}H\}$ NMR (150 MHz, $CDCl_3$): δ 169.3, 168.5, 56.2, 40.3, 38.6, 34.5, 30.9, 28.4, 25.7, 24.5 ppm.

PhB Anhydride

EDC·HCl (708 mg, 3.68 mmol) was added to a solution of 4-phenylbutyric acid (1.01 g, 6.14 mmol) in 10 mL chloroform. The reaction mixture was stirred overnight at room temperature. The next day, EDC·HCl (236 mg,

1.22 mmol) was added again to complete the reaction. After 2 h, the solution was washed with citric acid (1 g/100 mL) and $NaHCO_3$ (1 g/100 mL), dried over anhydrous Na_2SO_4 and dried in vacuum. The final product was stored in the freezer and yielded as white solid (786 mg, 82%). ^{1}H-NMR (400 MHz, $CDCl_3$); δ 7.32–7.28 (m, 2H), 7.23–7.17 (m, 3H), 2.70 (t, $J=7.6$, 2H, CH_2-CO), 2.45 (t, $J=7.4$, 2H, Ar-CH_2-), 2.04–1.96 (m, 2H, -CH_2-) ppm. ^{13}C{^{1}H} NMR (125 MHz, $CDCl_3$): δ 169.3, 141.0, 128.6, 128.6, 126.3, 34.8, 34.5, 25.8 ppm. EA: calculated for $C_{20}H_{22}O_3$: C, 77,39; H, 7.14%. Found: C, 77.09; H, 7.02%.

ALA Anhydride

A mixture of lipoic acid (109 mg, 0.53 mmol) and *N,N'*-dicyclohexylcarbodiimide (DCC, 60 mg, 0.29 mmol) in 5 ml of dichloromethane was kept stirring overnight at room temperature. The mixture solution was kept at −20 °C for complete precipitation of *N,N'*-dicyclohexylurea. The by-product was filtered off and the solution was dried under reduced pressure. A yellow oil was yielded (206 mg, 99%). The product was used for the next step directly without further purification.

cis,cis,trans-[Pt(NH$_3$)$_2$Cl$_2$(ALA)(OH)] **1**

Method A1. Oxoplatin (32 mg, 0.09 mmol) was added to a solution of ALA-NHS (30 mg, 0.10 mmol, 1.05 equiv.) in 3 ml of anhydrous DMSO. The suspension was heated to 50 °C and kept stirring under nitrogen overnight in the dark. The unreacted oxoplatin was removed through centrifuge. Excessive diethyl ether (2×40 ml) was added to remove DMSO. The residue was treated with dichloromethane to form a yellow precipitate, which was washed with dichloromethane and diethyl ether several times and dried under vacuum to receive complex **1** as yellow solid (20 mg, 40%).

Method B1. Oxoplatin (73 mg, 0.22 mmol) was added to a solution of freshly prepared ALA anhydride (79 mg, 0.20 mmol) in 6 ml of anhydrous DMF. The reaction mixture was stirred overnight at room temperature in the dark. Any insoluble solid was filtered off. DMF was removed by rotary evaporation and the residue was purified by column chromatography (SiO_2, MeOH/DCM = 1:10) to get complex **1** (16 mg, 15%).

^{1}H-NMR (400 MHz, (D_6)DMSO): δ 6.09–5.77 (m, 6H, 2×-NH_3), 3.64–3.57 (m, 1H, H_5), 3.22–3.09 (m, 2H, H_7), 2.46–2.38 (m, 1H, H_6), 2.17 (t, $J=6.0$, 2H, H_1), 1.93–1.85 (m, 1H, H_6), 1.72–1.63 (m, 1H, H_4), 1.59–1.34 (m, 5H, H_4/H_3/H_2) ppm. ^{13}C{^{1}H} NMR (100 MHz, (D_6)DMSO): δ 181.4, 56.7, 40.6, 38.5, 36.7, 34.7, 28.9, 25.9 ppm. ^{195}Pt{^{1}H} NMR (86 MHz, (D_6)DMSO): δ +1050 ppm. ESI-MS$^-$: *m/z* [M–H]$^-$ calc. for $C_8H_{19}N_2O_3Cl_2S_2Pt$: 520.9, found 520.8; *m/z* [M+Cl]$^-$ calc. for $C_8H_{20}N_2O_3Cl_3S_2Pt$: 556.9, found 556.7. EA: calculated for $C_8H_{20}N_2O_3Cl_2S_2Pt$: C, 18.39; H, 3.85; N, 5.36; S, 12.37%. Found: C, 18.37; H, 3.90; N, 5.85; S, 12.11%.

cis,cis,trans-[Pt(NH$_3$)$_2$Cl$_2$(ALA)$_2$] **2**

ALA anhydride (158 mg, 0.40 mmol) was added to a suspension of oxoplatin (33 mg, 0.10 mmol) in 5 ml of anhydrous DMF. The reaction mixture was stirred for 2 days at room temperature in the dark. The insoluble material was removed by centrifugation. The clear solution was evaporated to dryness in a rotary evaporator and the residue was purified by column chromatography (SiO_2, MeOH/DCM = 1:10) to get complex **2** (20 mg, 28%) as a yellow solid.

^{1}H-NMR (400 MHz, (D_6)DMSO): δ 6.50 (m, 6H), 3.62–3.56 (m, 2H), 3.22–3.09 (m, 4H), 2.48–2.40 (m, 2H), 2.23 (m, 4H), 1.92–1.84 (m, 2H), 1.71–1.63 (m, 2H), 1.58-1.37 (m, 10H) ppm. ^{13}C{^{1}H} NMR (75 MHz (D_6)DMSO): δ 181.1. 56.6, 38.5, 35.9, 34.6, 28.7, 27.1, 25.7 ppm. ^{195}Pt{^{1}H} NMR (76 MHz, (D_6)DMSO): δ +1230 ppm. ESI-MS$^-$: *m/z* [M–H]$^-$ calc. for $C_{16}H_{31}N_2O_4Cl_2S_4Pt$: 709.0, found 709.0. EA: calculated for $C_{16}H_{32}N_2O_4Cl_2S_4Pt$: C, 27.04; H, 4.54; N, 3.94; S, 18.05%. Found: C, 26.90; H, 4.34; N, 3.83; S, 18.11%.

cis,cis,trans-[Pt(NH$_3$)$_2$Cl$_2$(ALA)(PhB)] **3**

Method A2: PhB anhydride (124 mg, 0.80 mmol) was added to a suspension of **1** (67 mg, 0.20 mmol) in 2 ml of anhydrous DMF. The mixture was stirred overnight at room temperature. The clear solution, which was obtained through centrifugation, was dried by evaporation at reduced pressure. The resulted residue was treated with acetonitrile to form a yellow precipitation, which was washed with acetonitrile and diethyl ether several times and dried in vacuo to receive complex **3** as yellow solid (40 mg, 30%).

Method B2: Oxoplatin (69 mg, 0.21 mmol) was added to a solution of PhB anhydride (62 mg, 0.20 mmol) in 7 ml of DMSO. The mixture solution was stirred overnight at room temperature in the dark. The insoluble solid was filtered off to get a yellow solution. ALA anhydride (83 mg, 0.21 mmol) was added to the

filtrate and the mixture was kept stirring for 3 days at room temperature in the dark. DMSO was removed by addition of diethyl ether and the residue was purified by column chromatography (SiO_2, MeOH/DCM = 1:20) to get compound **3** (30 mg, 22%) as yellow solid.

^{1}H-NMR (400 MHz, (D_6)DMSO): δ 7.30–7.15 (m, 5H, H_{11}), 6.53 (br. s, 6H, 2×-NH_3), 3.64–3.57 (m, 1H, H_5), 3.22–3.09 (m, 2H, H_7), 2.59 (t, J = 8.0, 2H, H_{10}), 2.46–2.38 (m, 1H, H_6), 2.25–2.20 (m, 4H, H_1/H_8), 1.93–1.85 (m, 1H, H_6), 1.75 (quint, 2H, H_9), 1.70–1.63 (m, 1H, H_4), 1.57–1.34 (m, 5H, H_2/H_3/H_4) ppm. ^{13}C{^{1}H} NMR (100 MHz, (D_6)DMSO): δ 181.2, 181.0, 142.5, 128.9, 128.7, 126.1, 56.7, 40.9, 38.5, 36.0, 35.5, 34.9, 34.6, 28.7, 28.0, 25.7 ppm. ^{195}Pt NMR{^{1}H} (76 MHz, (D_6)DMSO): δ +1228 ppm. ESI-MS$^-$: *m/z* $[M–H]^-$ calc. for $C_{18}H_{29}N_2O_4Cl_2S_2Pt$: 667.0, found 666.8. EA: calculated for $C_{18}H_{30}N_2O_4Cl_2S_2Pt$: C, 32.33; H, 4.52; N, 4.19; S, 9.59%. Found: C, 32.18; H, 4.85; N, 3.74; S, 10.01%.

Electrochemistry

The measurements were performed on a Reference 600 Potentiostat (Gamry Instruments) using a three-electrode system consisting of glassy carbon (diameter 1.6 mm) as working electrode, Ag/Ag^+ in MeCN as reference electrode, and Pt wire as counter electrode. Corrections for the iR drop were performed for the experiments. All measurements were conducted in anhydrous DMF-[n-Bu_4N][PF_6] (0.1 M) solutions with a substance concentration of 1.0 mM at room temperature. The glassy carbon electrode was polished with alumina and the solutions were bubbled with nitrogen, prior to each measurement. During the measurements, the nitrogen stream was maintained over the solutions. Potential values presented here were calculated by referencing the potential of the ferrocenium/ferrocene (Fc^+/Fc) couple.

Reduction Study

Complexes **1** and **3** (16 mM) were mixed with ascorbic acid (5 equiv.) in DMF-PBS buffer (pH 7.4; 4:1). The solutions were incubated at 37 °C. ^{195}Pt{^{1}H} NMR spectra were measured at different incubation times.

DNA Interaction

Complex **1** (16 mM) was reacted with 9MeG (3 equiv.) in the presence of AsA (5 equiv.) in DMF-PBS (pH 7.4; 4:1) at 37 °C for 20 h. Cisplatin (16 mM) and 9MeG (3 equiv.) were incubated in DMF-PBS (pH 7.4; 4:1) at 37 °C for 20 h.

Cell Cultivation

SW480 (colon carcinoma) and A549 (non-small-cell lung carcinoma) cells were supplied by the Institute of Cancer Research, Department of Medicine I, Medical University of Vienna, Austria. CH1/PA-1 (ovarian teratocarcinoma) cells were donated by Lloyd R. Kelland, CRC Center for Cancer Therapeutics, Institute of Cancer Research, Sutton, UK. The cell lines were cultured in Minimal Essential Medium (MEM) containing 1 mM sodium pyruvate, 4 mM l-glutamine, 1% non-essential amino acids from 100× ready-to-use stock (all purchased from Sigma–Aldrich (Austria)) and 10% heat-inactivated fetal bovine serum (FBS, from Biowest) in 75 cm^2 culture flasks from CytoOne (Starlab, UK). Cells were grown under incubation at 37 °C and 5% CO_2 in a humidified atmosphere.

MTT Assay

Cells were trypsinized by using trypsin-EDTA (Sigma–Aldrich), counted, seeded into 96-well plates (SW480: 2000 cells per well; A549: 3000 cells per well; CH1/PA-1: 1000 cells per well, each in 100 µL) and incubated for 24 h at 37 °C and 5% CO_2. The Pt(IV) complexes were dissolved in DMSO, cisplatin and lipoic acid in supplemented MEM and serially diluted to different concentrations that were added in volumes of 100 µL onto the cells and incubated for 96 h at 37 °C. Afterwards, the cells were treated with 100 µL 3-(4,5-dimethylthiazol-2-yl)-2,5-diphenyl-2*H*-tetrazolium bromide (MTT) solution (0.6 mol/L in RPMI1640 medium containing 10% heat-inactivated FBS and 4 mM L-glutamine) per well and incubated for 4 h at 37 °C. 150 µL DMSO per well were used to dissolve the formazan crystals. Plates were measured at 550 nm (absorption maximum of formazan) and 690 nm (reference) with a microplate reader (BioTek ELx808), and IC_{50} values were interpolated by using Gen5™ software (BioTek). At least three biologically independent experiments were performed, each of them containing three replicates per concentration.

ROS Assay

SW480 cells were trypsinized, counted, seeded into 96-well-plates (25,000 cells per well in 100 µL) and preincubated for 24 h at 37 °C and 5% CO_2. The wells were washed with Hanks' Balanced Salt Solution

(HBSS) containing 1% FBS and cells were treated with 100 μL of 25 μM 2′,7′-dichlorofluorescein diacetate (DCFH-DA) solution in HBSS (1% FBS) for 45 min at 37 °C and washed with 200 μL HBSS (1% FBS). The complexes and *tert*-butyl peroxide (400 μM) as positive control were serially diluted in phenol-red-free MEM (1% FBS). After incubation with DCFH-DA, cells were washed two times with 200 μL HBSS (1% FBS), afterwards treated with the substances as well as the positive control. The positive control was used to exemplify the staining efficiency (*Figure S17*). For representation, the values were calculated as ratio between the means of the treated samples and the means of the untreated, negative control. The development of fluorescence was measured over 2 h every 10 min with the Synergy HT reader (BioTek; excitation: 485/20 nm, emission: 516/20 nm.

Acknowledgements

This work was supported by a grant from China Scholarship Council (CSC). Also, we would like to thank the financial support from Erasmus Plus Programme for a visiting research fellowship. We are thankful to Umicore AG & Co. KG Hanau – Wolfgang, Germany for the generous loan of potassium tetrachloroplatinate(II) compound. Open Access funding enabled and organized by Projekt DEAL.

Data Availability Statement

The data that support the findings of this study are available in the supplementary material of this article.

Author Contribution Statement

X. L. and M.-C. B. performed the experiments, analyzed the data and wrote the article. K. C. and M. A. J. supervised the biological tests. C. R. K., B. K. K., D. G. and W. W. mentored the project. All authors read and affirmed the manuscript.

References

[1] L. J. Reed, B. G. DeBusk, I. C. Gunsalus, C. S. Hornberger, 'Crystalline a-lipoic acid: A Catalytic Agent Associated with Pyruvate Dehydrogenase', *Science* **1951**, *114*, 93–94.
[2] L. Packer, E. Cadenas, 'Lipoic acid: energy metabolism and redox regulation of transcription and cell signaling', *J. Clin. Biochem. Nutr.* **2011**, *48*, 26–32.
[3] D. Tibullo, G. Volti, C. Giallongo, S. Grasso, D. Tomassoni, C. Anfuso, G. Lupo, F. Amenta, R. Avola, V. Bramanti, 'Biochemical and clinical relevance of alpha lipoic acid: antioxidant and anti-inflammatory activity, molecular pathways and therapeutic potential', *Inflammation Res.* **2017**, *66*, 947–959.
[4] B. Salehi, Y. B. Yilmaz, G. Antika, T. B. Tumer, M. F. Mahomoodally, D. Lobine, M. Akram, M. Riaz, E. Capanoglu, F. Sharopov, N. Martins, W. C. Cho, J. Sharifi-Rad, 'Insights on the Use of α-Lipoic Acid for Therapeutic Purposes', *Biomol. Eng.* **2019**, *9*, 356.
[5] A. M. Usacheva, A. V. Chernikov, E. E. Karmanova, V. I. Bruskov, 'Pharmacological Aspects of the Use of Lipoic Acid (Review)', *Pharm. Chem. J.* **2022**, *55*, 1138–1146.
[6] B. Dörsam, J. Fahrer, 'The disulfide compound α-lipoic acid and its derivatives: A novel class of anticancer agents targeting mitochondria', *Cancer Lett.* **2016**, *371*, 12–19.
[7] P. Theodosis-Nobelos, G. Papagiouvannis, P. Tziona, E. A. Rekka, 'Lipoic acid. Kinetics and pluripotent biological properties and derivatives', *Mol. Biol. Rep.* **2021**, *48*, 6539–6550.
[8] A. Diane, N. Mahmoud, I. Bensmail, N. Khattab, H. A. Abunada, M. Dehbi, 'Alpha lipoic acid attenuates ER stress and improves glucose uptake through DNAJB3 cochaperone', *Sci. Rep.* **2020**, *10*, 20482.
[9] A. Solmonson, R. J. DeBerardinis, 'Lipoic acid metabolism and mitochondrial redox regulation', *J. Biol. Chem.* **2018**, *293*, 7522–7530.
[10] B. Feuerecker, S. Pirsig, C. Seidl, M. Aichler, A. Feuchtinger, G. Bruchelt, R. Senekowitsch-Schmidtke, 'Lipoic acid inhibits cell proliferation of tumor cells in vitro and in vivo', *Cancer Biol. Ther.* **2012**, *13*, 1425–1435.
[11] L. G. Korotchkina, S. Sidhu, M. S. Patel, 'R-Lipoic Acid Inhibits Mammalian Pyruvate Dehydrogenase Kinase', *Free Radical Res.* **2004**, *38*, 1083–1092.
[12] D. Farhat, H. Lincet, 'Lipoic acid a multi-level molecular inhibitor of tumorigenesis', *Biochim. Biophys. Acta Rev. Cancer* **2020**, *1873*, 188317.
[13] N. A. G. dos Santos, R. S. Ferreira, A. C. d Santos, 'Overview of cisplatin induced neurotoxicity and ototoxicity, and the protective agents', *Food Chem. Toxicol.* **2020**, *136*, 111079.
[14] N. Pınar, G. Çakırca, S. Hakverdi, M. Kaplan, 'Protective effect of alpha lipoic acid on cisplatin induced hepatotoxicity in rats', *Biotech. Histochem.* **2019**, *95*, 219–224.
[15] K.-H. Kim, B. Lee, Y.-R. Kim, M.-A. Kim, N. Ryu, D. J. Jung, U.-K. Kim, J.-I. Baek, K.-Y. Lee, 'Evaluating protective and therapeutic effects of alpha-lipoic acid on cisplatin-induced ototoxicity', *Cell Death Dis.* **2018**, *9*, 827.
[16] N. J. Wheate, S. Walker, G. E. Craig, R. Oun, 'The status of platinum anticancer drugs in the clinic and in clinical trials', *Dalton Trans.* **2010**, *39*, 8113–8127.

[17] S. Dilruba, G. V. Kalayda, 'Platinum-based drugs: past, present and future', *Cancer Chemother. Pharmacol.* **2016**, *77*, 1103–1124.
[18] S. Rottenberg, C. Disler, P. Perego, 'The rediscovery of platinum-based cancer therapy', *Nature Rev.* **2021**, *21*, 37–50.
[19] T. C. Johnstone, K. Suntharalingam, S. J. Lippard, 'The Next Generation of Platinum Drugs: Targeted Pt(II) Agents, Nanoparticle Delivery, and Pt(IV) Prodrugs', *Chem. Rev.* **2016**, *116*, 3436–3486.
[20] R. Oun, Y. E. Moussa, N. J. Wheate, 'The side effects of platinum-based chemotherapy drugs: a review for chemists', *Dalton Trans.* **2018**, *47*, 6645–6653.
[21] S. Ivanova, 'Comparative assessment of clinical trials, indications, pharmacokinetic parameters and side effects of approved platinum drugs', *Pharmacia* **2022**, *69*, 1–7.
[22] D. Gibson, 'Platinum(IV) anticancer prodrugs – hypotheses and facts', *Dalton Trans.* **2016**, *45*, 12983–12991.
[23] Z. Xu, Z. Wang, Z. Deng, G. Zhu, 'Recent advances in the synthesis, stability, and activation of platinum(IV) anticancer prodrugs', *Coord. Chem. Rev.* **2021**, *442*, 213991.
[24] D. Gibson, 'Platinum(IV) anticancer agents; are we en route to the holy grail or to a dead end?', *J. Inorg. Biochem.* **2021**, *217*, 111353.
[25] M. Ravera, E. Gabano, M. J. McGlinchey, D. Osella, 'Pt(IV) antitumor prodrugs: dogmas, paradigms, and realities', *Dalton Trans.* **2022**, *51*, 2121–2134.
[26] D. Gibson, 'Pt(IV) Anticancer Prodrugs – A Tale of Mice and Men', *ChemMedChem* **2021**, *16*, 2188–2191.
[27] D. Gibson, 'Multi-action Pt(IV) anticancer agents; do we understand how they work?', *J. Inorg. Biochem.* **2019**, *191*, 77–84.
[28] R. Raveendran, J. P. Braude, E. Wexselblatt, V. Novohradsky, O. Stuchlikova, V. Brabec, V. Gandin, D. Gibson, 'Pt(IV) derivatives of cisplatin and oxaliplatin with phenylbutyrate axial ligands are potent cytotoxic agents that act by several mechanisms of action', *Chem. Sci.* **2016**, *7*, 2381–2391.
[29] P. W. Atadja, 'HDAC inhibitors and cancer therapy', *Prog. Drug Res.* **2011**, *67*, 175–195.
[30] M. J. Lee, Y. S. Kim, S. Kummar, G. Giaccone, J. B. Trepel, 'Histone deacetylase inhibitors in cancer therapy', *Curr. Opin. Oncol.* **2008**, *20*, 639–649.
[31] S. Savino, C. Marzano, V. Gandin, J. D. Hoeschele, G. Natile, N. Margiotta, 'Multi-Acting Mitochondria-Targeted Platinum(IV) Prodrugs of Kiteplatin with α-Lipoic Acid in the Axial Positions', *Int. J. Mol. Sci.* **2018**, *19*, 2050.
[32] M. D. Hall, C. T. Dillon, M. Zhang, P. Beale, Z. Cai, B. Lai, A. P. J. Stampfl, T. W. Hambley, 'The cellular distribution and oxidation state of platinum(II) and platinum(IV) antitumour complexes in cancer cells', *J. Biol. Inorg. Chem.* **2003**, *8*, 726–732.
[33] D. A. Tolan, Y. K. Abdel-Monem, M. A. El-Nagar, 'Anti-tumor platinum (IV) complexes bearing the anti-inflammatory drug naproxen in the axial position', *Appl. Organomet. Chem.* **2019**, *33*, e4763.
[34] L. Shi, C. Jing, W. Ma, D.-W. Li, J. E. Halls, F. Marken, Y.-T. Long, 'Plasmon Resonance Scattering Spectroscopy at the Single-Nanoparticle Level: Real-Time Monitoring of a Click Reaction', *Angew. Chem. Int. Ed.* **2013**, *52*, 6011–6014; *Angew. Chem.* **2013**, *125*, 6127–6130.
[35] A. Sadownik, J. Stefely, S. L. Regen, 'Polymerized Liposomes Formed under Extremely Mild Conditions', *J. Am. Chem. Soc.* **1986**, *108*, 7789–7791.
[36] N. Muhammad, N. Sadia, C. Zhu, C. Luo, Z. Guo, X. Wang, 'Biotin-tagged platinum(IV) complexes as targeted cytostatic agents against breast cancer cells', *Chem. Commun.* **2017**, *53*, 9971–9974.
[37] J. Z. Zhang, E. Wexselblatt, T. W. Hambley, D. Gibson, 'Pt(IV) analogs of oxaliplatin that do not follow the expected correlation between electrochemical reduction potential and rate of reduction by ascorbate', *Chem. Commun.* **2012**, *48*, 847–849.
[38] Z. Xu, H. Chan, C. Li, Z. Wang, M. Tse, Z. Tong, G. Zhu, 'Synthesis, Structure, and Cytotoxicity of Oxaliplatin-Based Platinum(IV) Anticancer Prodrugs Bearing One Axial Fluoride', *Inorg. Chem.* **2018**, *57*, 8227–8235.
[39] D. Tolan, V. Gandin, L. Morrison, A. El-Nahas, C. Marzano, D. Montagner, A. Erxleben, 'Oxidative Stress Induced by Pt(IV) Pro-drugs Based on the Cisplatin Scaffold and Indole Carboxylic Acids in Axial Position', *Sci. Rep.* **2016**, *6*, 29367.
[40] E. Wexselblatt, D. Gibson, 'What do we know about the reduction of Pt(IV) pro-drugs?', *J. Inorg. Biochem.* **2012**, *117*, 220–229.
[41] T. Mosmann, 'Rapid Colorimetric Assay for Cellular Growth and Survival: Application to Proliferation and Cytotoxicity Assays', *J. Immunol. Methods* **1983**, *65*, 55–63.
[42] F. Denizot, R. Lang, 'Rapid colorimetric assay for cell growth and survival - Modifications to the tetrazolium dye procedure giving improved sensitivity and reliability', *J. Immunol. Methods* **1986**, *89*, 271–277.
[43] J. Tripathy, A. Tripathy, M. Thangaraju, M. Suar, S. Elangovan, 'α-Lipoic acid inhibits the migration and invasion of breast cancer cells through inhibition of TGFβ signaling', *Life Sci.* **2018**, *207*, 15–22.
[44] A. Kuban-Jankowska, M. Gorska-Ponikowski, M. Wozniak, 'Lipoic acid decreases the viability of breast cancer cells and activity of PTP1B and SHP2', *Anticancer Res.* **2017**, *37*, 2893–2898.
[45] I. Damnjanovic, G. Kocic, S. Najman, S. Stojanovic, D. Stojanovic, A. Veljkovic, I. Conic, T. Langerholc, S. Pesic, 'Chemopreventive potential of alpha lipoic acid in the treatment of colon and cervix cancer cell lines', *Bratisl. Lek. Listy* **2014**, *115*, 611–616.
[46] L. Packer, E. H. Witt, H. J. Tritschler, 'Alpha-Lipoic Acid as a Biological Antioxidant', *Free Radical Biol. Med.* **1995**, *19*, 227–250.
[47] G. P. Biewenga, G. R. M. M. Haenen, A. Bast, 'The Pharmacology of the Antioxidant Lipoic Acid', *Gen. Pharmacol.* **1997**, *29*, 315–331.
[48] G. Simbula, A. Columbano, G. M. Ledda-Columbano, L. Sanna, M. Deidda, A. Diana, M. Pibiri, 'Increased ROS generation and p53 activation in α-lipoic acid-induced apoptosis of hepatoma cells', *Apoptosis* **2007**, *12*, 113–123.
[49] H. Moini, L. Packer, N. E. L. Saris, 'Antioxidant and Prooxidant Activities of α-Lipoic Acid and Dihydrolipoic Acid', *Toxicol. Appl. Pharmacol.* **2002**, *182*, 84–90.
[50] P. D. Ray, B.-W. Huang, Y. Tsuji, 'Reactive oxygen species (ROS) homeostasis and redox regulation in cellular signaling', *Cell. Signalling* **2012**, *24*, 981–990.
[51] N. Ghosh, A. Das, S. Chaffee, S. Roy, C. K. Sen, *Immunity and Inflammation in Health and Disease - Emerging Roles of*

Nutraceuticals and Functional Foods in Immune Support, Academic Press, San Diego, **2017**.
[52] B. Perillo, M. Di Donato, A. Pezone, E. Di Zazzo, P. Giovannelli, G. Galasso, G. Castoria, A. Migliaccio, 'ROS in cancer therapy: the bright side of the moon', *Exp. Mol. Med.* **2020**, *52*, 192–203.
[53] T. Zaidieh, J. R. Smith, K. E. Ball, Q. An, 'ROS as a novel indicator to predict anticancer drug efficacy', *BMC Cancer* **2019**, *19*, 1224.
[54] H. Yang, R. M. Villani, H. Wang, M. J. Simpson, M. S. Roberts, M. Tang, X. Liang, 'The role of cellular ROS in cancer chemotherapy', *J. Exp. Clin. Cancer Res.* **2018**, *37*, 266.
[55] S. Mirzaei, A. Mohammadi, M. Gholami, F. Hashemi, A. Zarrabi, A. Zabolian, K. Hushmandi, P. Makvandi, M. Samec, A. Liskova, P. Kubatka, N. Nabavi, A. Aref, M. Ashrafizadeh, H. Khan, M. Najafi, 'Nrf2 signaling pathway in cisplatin chemotherapy: Potential involvement in organ protection and chemoresistance', *Pharmacol. Res.* **2021**, *167*, 105575.
[56] D. Xue, X. Zhou, J. Qiu, 'Emerging role of NRF2 in ROS-mediated tumor chemoresistance', *Biomed. Pharmacother.* **2020**, *131*, 110676.
[57] H. Kim, X. Xue, 'Detection of Total Reactive Oxygen Species in Adherent Cells by 2',7'-Dichlorodihydrofluorescein Diacetate Staining', *J. Visualization* **2020**, *160*, e60682.

Received July 24, 2022
Accepted August 26, 2022

